MINERALOGY OF SHEARED SERPENTINITE NEAR MLAKAWA MOUNTAIN, PENJWIN DISTRICT, KURDISTAN REGION, NE IRAQ

Yousif O. Mohammad[*] and Irfan O. Mousa[**]

Received: 3/ 11/ 2008, Accepted: 9/ 6/ 2009

ABSTRACT

Shear serpentinite represents two meters thick serpentinite, formed at the contact of the Penjween Ophiolite sequence and Tertiary molasses (Miocene Merga Red Beds). It is formed of metamorphism of massive serpentinite as a result of Tertiary post-collision tectonics. Mineralogically, shear serpentinite consists of serpentine polymorphs mainly antigorite, lizardite – chrysotile serpentines, bands of carbonate minerals, subordinate amount of magnetite. There are two types of the later: **a)** chemically zoned large grains with cores of primary Cr-spinel and/ or pre-serpentanization ferrichromites; and **b)** small, unzoned, pure syn-serpentanization magnetite grains. The first type of magnetite occupies the outermost of rimmed Cr-spinel. Lizardite – chrysotile fibers enclose strips within antigorite suggesting that it formed on expense of this mixture of chrysotile and lizardite. Antigorite is formed under shear stress condition during post-collision tectonics. Chemical analysis of serpentine polymorphs shows that the antigorite is richer in FeO and poorer in MgO and SiO_2 than that in lizardite – chrysotile serpentines. The co-existing of high-Fe antigorite with lizardite – chrysotile assemblage may suggest that the earlier is stable in slightly higher temperature condition (>300° C) than that of lizardite and chrysotile serpentine. Back scattered images (BSE) show that antigorite is granular light gray, whereas the lizardite – chrysotile is fibrous dark gray. Chlorite is a Cr-rich clniochlorite (2.6 wt.% Cr_2O_3). It is formed through the reaction of ferrichromite with serpentine minerals during retrograde metamorphism. The occurrence of this shear serpentine along post-collision strike – slip fault zones suggests that they used these zones of weakness for protrusion.

معدنية صخور السربنتينايت القصية
قرب جبل ملةكوة، منطقة بنجوين، إقليم كردستان، شمال شرق العراق

يوسف عثمان محمد و عرفان عمر موسى

المستخلص

تتمثل صخور السربنتينايت القصية بسمك مترين من السربنتينايت التي تقع على الفالق الزاحف الرئيسي الواقع بين تتابع بنجوين الاوفيولايتي وسلسلة الطبقات الحمراء. وقد تكونت هذه الصخور خلال التحول التقادمي لصخور السربنتينايت الكتلية نتيجة للارتفاع الموضعي للضغط والحرارة خلال زحف تتابع اوفيولايت بنجوين على الحافة الشمالية الشرقية للصحيفة العربية في العصر الثلاثي. معدنياً يتكون السربنتين القصي من السربنتين متعدد الأشكال والذي يتكون بشكل رئيسي من انتيكورايت وليزيردايت - كريزوتايل وأحزمة من المعادن الكلسية وعروق ثانوية من المكنيتايت المصاحب لعملية السربنتنة المشتق من معدني الأوليفين والبايروكسين المتحولين الى السربنتين. وتحتوي صخور السربنتينايت كذالك على المكنيتايت المحتوي على الكروم ذات البلورات كاملة الأوجه والبلورات

[*] Department of Geology, University of Sulaimaniyah, Kurdistan Region, Iraq. e-mail: yousif_geo76@yahoo.com

[**] Department of Geology, University of Sulaimaniyah, Kurdistan Region, Iraq. e-mail: Eirfan2004@yahoo.co.uk

شبه كاملة الأوجه المشتقة من معدن السبينيل الكرومي مع وجود الكلورايت الكرومي أيضاً. يوجد معدن الانتيكورايت على شكل حبيبات ضمن الياف الليزردايت - الكريزوتايل وهذا يدل على ان المعدن تكون بواسطة عملية إعادة التبلور أثناء عملية التحول التقدمي الليزردايت - الكريزوتايل. ان التحليل الكيميائي للسربنتين متعدد الأشكال يبين بان الانتيكورايت يحتوي على نسبة كبيرة من أوكسيد الحديد ونسبة قليلة من أوكسيد المغنيسيوم والسليكا مقارنةً بمعدن الليزردايت - الكريزوتايل. ويظهر هذا المعدن في الصور الخلفية المتشتتة كحبيبات ذات لون رصاصي فاتح بينما يكون الليزردايت - الكريزوتايل على شكل ألياف داكنة اللون. في هذا النوع من الصخور يوجد معدن الكلورايت مائل المحاور والذي يحتوي على نسبة وزنية تصل الى 2.6% وهو ناتج تفاعلي بين معدن السبينيل الكرومي مع أطوار السليكا خلال التفاعلات الذوبانية المائية للجزء العلوي من الجبة. وبشكل آخر يمكن لمعدن الكلورايت ان يتكون نتيجة تفاعل معدن الكرومايت الحديديكي مع معدن السربنتين خلال عمليات التحول الواطئ.

INTRODUCTION

Serpentinite has an important part to play in the local tectonic problems of the Iraqi Zagros Suture Zone (IZSZ). This is because serpentinite has low density (2.75 g/cm^3) and low viscosity (<1020 Pa.s.), acts as a highly lubricant and easily weathered (Mohammad and Maekawa, 2007). Aziz (2008) based on the field evidence and Sr-Nd isotopic data subdivided serpentinite of IZSZ into highly sheared serpentinite, which occupies lower contact of the ophiolitic sequence (Upper Allochthonous) (97 – 118 Ma ?) and ophiolitic mélange (refer to as a meta-ultramafic mélange) on the base of the Lower Allochthonous nap (Aswad, 1999). Through the pre-collision tectonic mélange (refer to as a meta-ultramafic mélange) and the allochthonous Qulqula radiolarite (sedimentary mélange), and the allochthonous Wallash volcano-sedimentary Series volcanites (32 – 42 Ma, see Koyi, 2006) along IZSZ. In post-collision tectonics, the allochthonous slabs finally overlain on Tertiary molasses (Tertiary sedimentary cover) by gravity sliding (Aswad, 1999). The radiometric age of massive serpentinite near Mlakawa mountain (Aziz, 2008), obtained by Rb-Sr methods (80 Ma?) correlated positively with K-Ar age (97 C 118 Ma) (Albian – Cenomanian) of subvolcanic rock of Mawat Ophiolite complex (Aswad and Elias, 1988). Based on inferred incorporation ages of units structurally above and below shear zone, shear serpentinite probably formed less than 30 Ma ago.

The oxygen and hydrogen isotopic compositions of serpentinite near Mlakawa (Mohammed, 2004 and Aqrawi *et al.,* 2007) are reported in standard δ notation relative to Standard Mean Ocean Water (SMOW), show $\delta 10^{18}$ = (10.90 – 13.29) % and δD = (– 69 to – 74) %. Based on the isotopic δD and δ^{18}O available data may suggest that the serpentinization was resulted of interaction of water from dehydration of down going slab with olivine (i.e. internally buffer interaction) at temperature 150° C and 300° C (Mohammed, 2004).

Massive Serpentinite, in the studied area, are from the metamorphism of dunite and harzburgite as blocky resistant rocks that crop out in Mlakawa mountain near Kani Manga village with a total thickness of (100 – 200) m. Sheared serpentinite of two meter thick, was found at the contact separating Penjween Ophiolite sequence and Miocene Merga Red Beds. The absence of dynamo thermal sole in tectonic contact between the shear serpentinite and the Tertiary molasses (Miocene Merga Red Beds), which would normally have formed at the inception of the subduction (Nicolas *et al*., 1981), can be interpreted as a result of Miocene post-collision tectonics in which the boundary is allochthonous slab (Penjween Ophiolitic sequence) with Tertiary molasses.

Mineralogically, shear serpentinite consists mainly of serpentine polymorphs, with subordinate amount of bands of carbonate minerals, and syn-serpentinization magnetite formed after serpentinization of olivine and pyroxene. The studied serpentinite is characterized by anhedral to sudhedral primary Cr-spinel compositions, which have been

partly or completely obscured by a veil of pre- and syn- or post-serpentinization metamorphic effects.

Mineralogical properties of serpentine bearing rocks are poorly understood especially at large strains. Therefore, the aim of this study is to identify serpentine polymorphs in shear serpentinite near Mlakawa mountain in Kurdistan Region of NE Iraq. As well as related mineralogical assemblage of the shear serpentinite using extensive electron microprobe analyses and back scattered image analyses of serpentine mineral associates.

PREVIOUS STUDIES

Although the Penjween igneous complex was investigated by many geologist of the State Company of Geological Survey and Mining, most of them gave different ideas concerning the stratigraphy, structure and age of the complex. Detailed data regarding petrology, mineralogy and geochemistry of serpentinite is still lacking.

The first geological map of the area was compiled by McCarthy (1956). In addition, he gave a brief field description of various rock units of the area and he reported that the Penjween igneous complex consists of ultrabasic, basic and intermediate rocks intruded to phyllite, calc-schist and marbles.

Simrnove and Nelidove (1962) suggested that the ultrabasic and basic rocks in Penjween area represent laccolith-like body, which were confined in an anticlinal core that composed of marble and schist, and they postulated that the igneous massive was an in site intrusive body.

Al-Hassan (1975) studied both Mawat and Penjween complexes, and he concluded that both complexes were differentiated from the same magma source.

Mahmmod (1978) studied the ultramafic and associated chromite in Penjween area; she concluded that the ultramafic rocks consist of harzburgite, dunite, lherzolite and pyroxenite. As well as she regarded that Penjween igneous complex is an alpine type ultramafic rocks.

Al-Hassan (1982) concluded that Penjween igneous complex is incomplete ophiolite suite and was originated from marginal basin developed in the Late Cretaceous.

Mohammad (2004) studied the serpentinite associated with ophiolite; he identified three types of serpentinite (massive, shear and veinlet). Also he conclude that the serpentinization processes of Penjween ultramafic rock was allochemical process and formed by interaction of oceanic water with basal harzburgite part of ophiolite suite.

ANALYTICAL TECHNIQUES

The samples of this study were collected near village of Kani Manga, which is located 60 Km NE of Sulaimaniyah city. Shear serpentinite croups out along the main road that connects between Sulaimaniyah city and Penjween town. Chemical analyses of essential minerals were determined using JEOL-840A scanning electron microscope equipped with Oxford energy – dispersive detector (EDX), analytical system (Link ISIS series L200I-S) at Osaka Prefecture University in Japan. Accelerating voltage and current kept at 15.0 Kv and 0.5 nA, respectively, correction were made using ZAF method. Suitable synthetic and natural mineral standards were applied for calibration. Total iron was measured as FeO by microprobe and was recalculated on ideal stoichiometry to give the FeO and Fe_2O_3 value using the general equation of Droop (1987). For BSE study of serpentine polymorphs, the prepared thin sections thickness is less than standard thickness 0.3 mm by 0.05 mm.

FIELD OCCURRENCE AND PETROGRAPHY

Sheared serpentinite is two meters thick serpentinite that occur along the main thrust fault between Penjween Ophiolite sequence and Merga Red Beds (Fig.1). It is restricted to the periphery of the massive serpentinite and gradationally in warded to massive serpentinite.

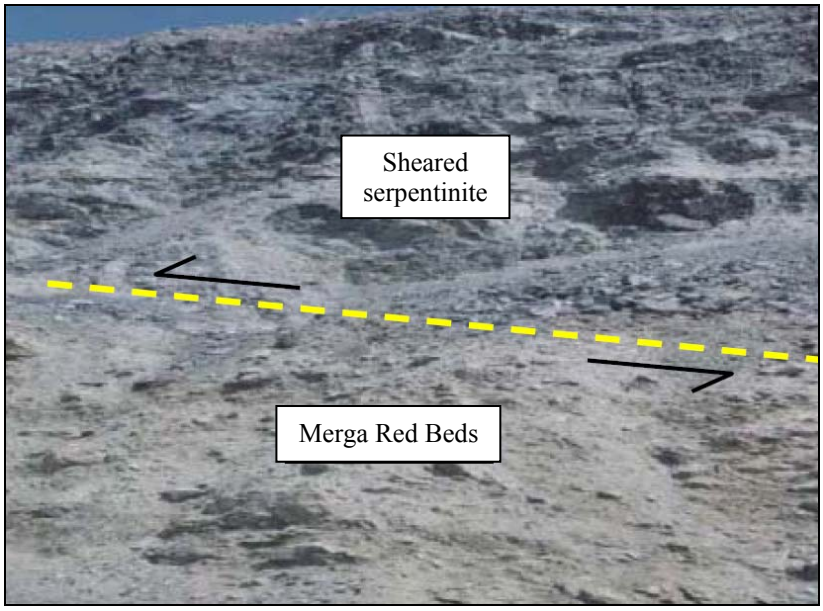

Fig.1: Tectonic thrust contact between sheared serpentinite and Merga Red Beds

Under thin section, the serpentinite shows a typical Tiger skin texture (Fig.2A) of white bands of carbonate minerals and bluish-gray bands of serpentine minerals. Serpentine minerals are commonly arranged in sub parallel alignments producing schistosity. Coarse grained serpentine minerals show effect of ductile deformation, like lamellar structure, bending and ellipsoidal shapes (Fig.2B). Syn-serpentinization magnetite occurs as a small discontineous veinlet parallel to the main schistosity direction (Fig.2C), or occurs as fine dusty grains within the chrysotile veins (Fig.2D). Disseminated chromian spinel occurs as highly fractured porphyroclasts usually shows the effect of ductile – brittle deformation (Fig.2E). Ductile deformation is represented by elongation of spinel grains parallel to the main schistosity direction, while brittle deformation is represented by fracturing and or splitting perpendicular to the main schistosity direction. Carbonate minerals occur as continuous bands among serpentine bands, some time show coarse crystalline vein filling dolomite with two set of cleavages (Fig.2F).

MINERAL CHEMISTRY AND BACK SCATTERD IMAGES

▪ Serpentine Minerals

The serpentine is referred to as a family name of lizardite, chrysotile and antigorite of serpentine polymorphs, with a general formula $Mg_3Si_2O_5(OH)_4$. Lizardite consists of planner layer, chrysotile of scrolled layer in which either *a* or *b* crystallographic axis coincides with axis of slender. Antigorite, however, is characterized by a superstructure with large periodicity (*m*-value = number of tetrahedral in a single chain along the wavelength *a*) along the *a* direction based on an alternating wave structure (Kunze, 1956 and 1958) (Fig.3). The later occurs widely across the low-grade to high-grade metamorphic domains. These wide metamorphic domains are attributed to the variations in super cell parameter (i.e. *m*-value) and chemical composition. According to Kunze (1958), compositional variations of antigorite can be expressed by the formula $M_{3m-3}T_2mO_5m(OH)_4m-_6$ (M= octahedral cations like Mg, Fe^{2+}, Ni, Al; T= tetrahedral cations like Si, Al, Fe^{3+}; *m* = number of tetrahedral in a single chain along wavelength *a*) (Fig.3). Fe^{2+}, however, is most common and tends to dominate over Fe^{3+}.

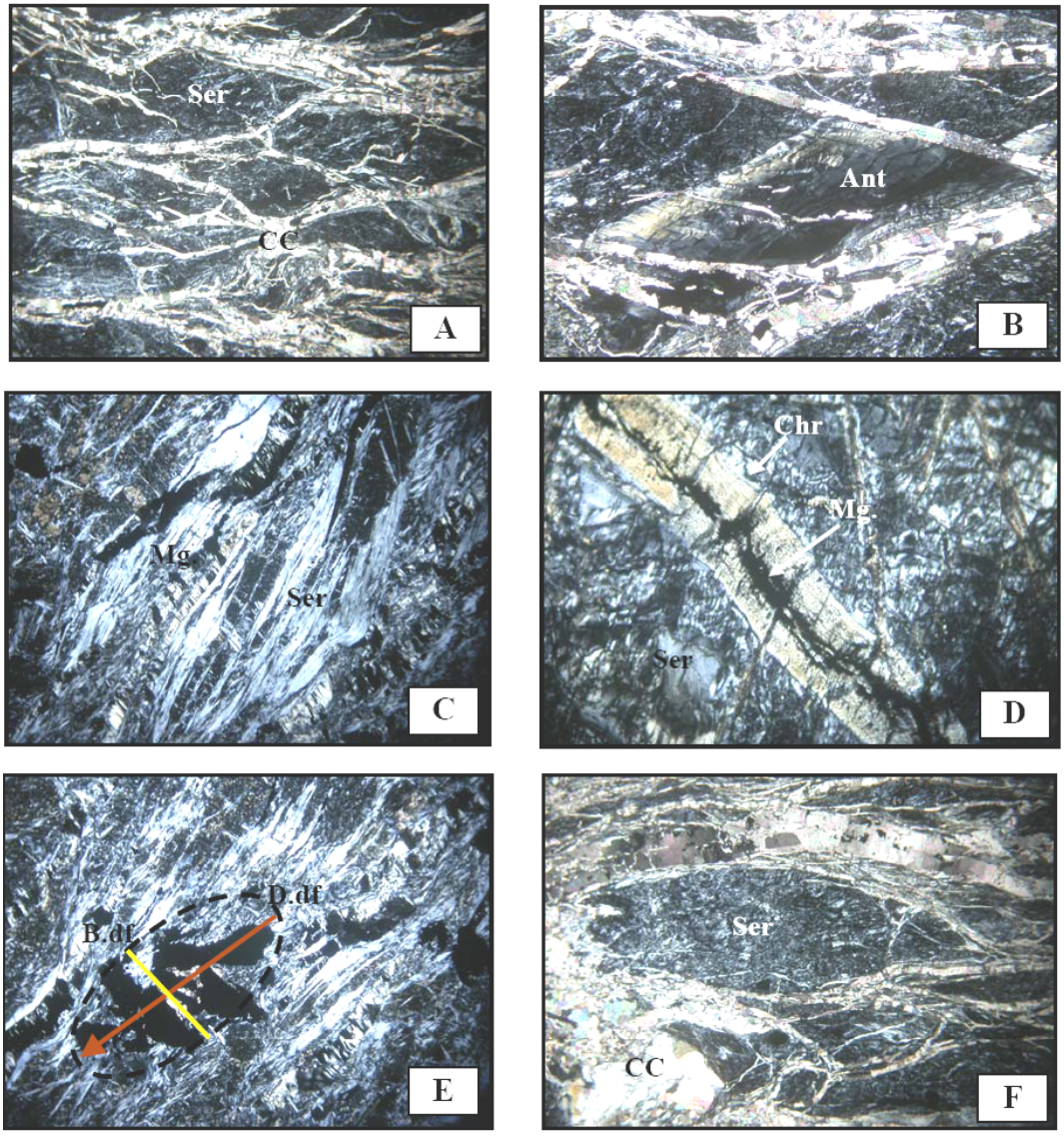

Fig.2: Photomicrographs of sheared serpentinite showing:

A) Tiger skin texture of sheared serpentinite (under XP)

B) Ductile deformation in serpentine minerals (under XP)

C) Magnetite veinlet arranged parallel to the main serpentine schistosity (under XP)

D) Fine grain dusty magnetite in the serpentine vein (under XP**)**

E) Ductile – brittle deformation in chromian spinel, the ductile deformation (elongation) is parallel to the main schistosity direction, while the brittle deformation is perpendicular to the main schistosity direction

F) Coarse grain calcite vein showing two sets of cleavage with ellipsoidal serpentine minerals (under XP).

Abbreviations: Ser = serpentine minerals; Ar = Aragonite; Ant = Antigorite; Mg = Magnetite; Cr-spl = Chromium spinel; D.df. = Ductile deformation phase and B.df = Brittle deformation phase in chromian spinel.

Chapman and Zussman (1959) observed *a* cell dimensions between 16.8 and 109 Å, which would correspond to *m*-values of 7 to 41. However, Mellini and Zussman (1986) discovered that "antigorites" of very low *a*-values between (16.8 and 33.7) Å were miss identifications of carlosturanite, which has the ideal formula $Mg_{42}Si_{24}O_{56}(OH)_{68}(H_2O)_2$. TEM-study carried out by Mellini *et al*. (1987) indicates a T-dependence of *m*-values. With increasing metamorphic grade of the serpentinite they observed a decrease of the *m*-value. Mellini *et al*. (1987) found that with increasing temperature, the antigorite become richer in SiO_2 and the super lattice periodicity (*m*-values) decrease from bout 6.0 nm at 250° C to about 3.5 nm at 550° C. The estimated *m*-value, i.e. *m* = [3 (3- (2 M/T)] of the studied antigorite is approximately equal to 10 nm. Furthermore, the *m*-value of antigorite is not only dependent on P and T, but also on additional factors: *e.g.* (1) the parageneses from which antigorite is formed, (2) the water activity during antigorite formation, (3) composition of antigorite (especially its iron content) (Wunder *et al*., 2001). FeO played a significant role in controlling the temperature of antigorite-forming reaction. Antigorite of lower Mg/ (Mg+Fe) ratio has lower metamorphic grade (Worden *et al*., 1991). In addition to the variations in super cell parameter (*m*-value) and chemical composition, antigorite formation required shear stress condition (Auzende *et al*., 2003).

Extensive chemical investigations (1000 point analyses) of the serpentine polymorphs have been performed in order to identify different serpentine polymorphs, only the representative analyses are shown in Table (1). The analyses show that the compositions of serpentine minerals is highly variable due to different generation of serpentine minerals in time spanning from 80 to less than 30 Ma, and recrystallization process during prograde metamorphism between serpentinite polymorph as recorded by Spear (1994) and OHanly (1992). From chemical data it is clear that the analyzed lizardite – chrysotile $(Mg_{5.583}Fe_{0.143})Si_{4.110}Al_{0.000}O_5(OH)_4$ are poor in FeO and richer in MgO than the antigorite $(Mg_{5.275}Fe_{0.323})Si_{4.153}Al_{0.000}O_5(OH)_4$. The MgO – SiO_2 diagram (Fig.4A and 4B) FeO – MgO (Fig.5A), and FeO – SiO_2 diagram (Fig.5B), show that the analyzed serpentine polymorphs located in both field of antigorite serpentine for analyzed antigorite and lizardite – chrysotile for the analyzed mixed lizardite – chrysotile serpentine.

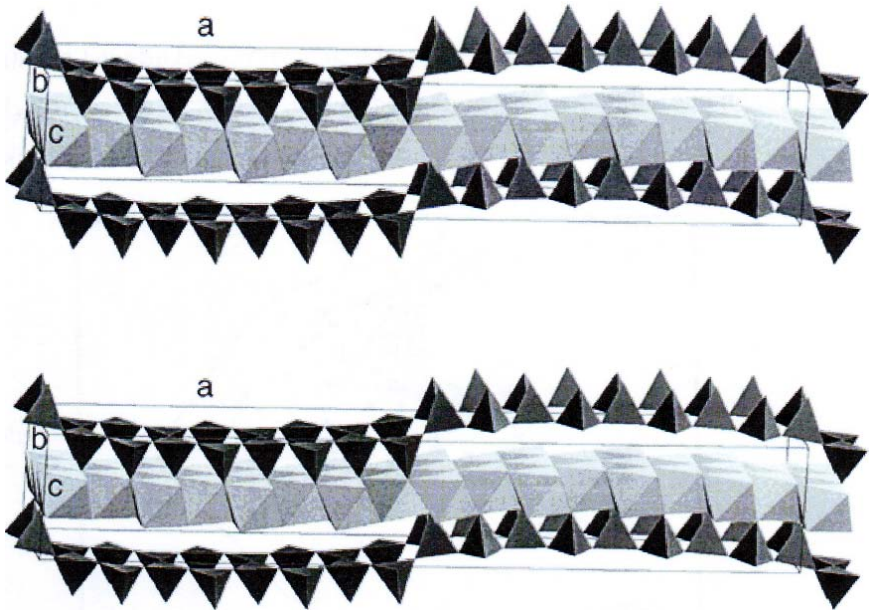

Fig.3: Crystal structure of antigorite with *m* = 17 (structural data from Uehara, 1998)

Table 1: Representative micro analyses of serpentine from sheared serpentinite

	Lizardite – Chrysotile								Antigorite				
Oxides (wt.%)													
SiO_2	44.60	45.76	45.96	44.84	44.75	46.10	45.58	45.65	45.53	46.13	45.02	46.04	46.00
TiO_2	0.01	0.00	0.08	0.00	0.06	0.10	0.07	0.06	0.00	0.04	0.00	0.00	0.00
Al_2O_3	0.00	0.00	0.00	0.04	0.87	0.49	0.17	0.62	0.09	0.00	0.00	0.00	0.00
Fe_2O_3	0.00	0.00	0.00	0.00	0.00	0.00	0.00	0.00	0.00	0.00	0.00	0.00	0.00
FeO	1.86	2.07	2.66	2.39	2.71	3.25	1.27	3.11	4.22	4.74	4.05	4.81	4.52
MnO	0.12	0.04	0.20	0.01	0.00	0.09	0.13	0.15	0.19	0.27	0.12	0.15	0.05
MgO	40.65	41.03	41.68	40.45	39.29	39.89	39.77	39.06	38.67	39.40	38.36	39.18	39.32
Cr_2O_3	0.38	0.00	0.07	0.05	0.05	0.00	0.00	0.09	0.03	0.00	0.01	0.00	0.14
V_2O_5	0.00	0.14	0.06	0.15	0.00	0.12	0.06	0.04	0.17	0.14	0.00	0.26	0.08
Total	87.66	89.05	90.78	87.93	87.74	89.92	87.01	88.74	88.84	90.62	87.66	90.18	90.03
Cation proportions per 14 oxygen atoms													
Si	4.110	4.138	33.405	4.117	4.121	4.146	4.194	4.161	4.167	4.153	4.179	4.157	4.162
Ti	0.001	0.000	0.044	0.000	0.004	0.007	0.005	0.004	0.000	0.003	0.000	0.000	0.000
Al	0.000	0.000	0.000	0.004	0.094	0.052	0.018	0.067	0.010	0.000	0.000	0.000	0.000
Fe^{3+}	0.000	0.000	0.000	0.000	0.000	0.000	0.000	0.000	0.000	0.000	0.000	0.000	0.000
Fe^{2+}	0.143	0.157	1.617	0.183	0.209	0.244	0.098	0.237	0.323	0.357	0.314	0.363	0.342
Mn	0.009	0.003	0.123	0.001	0.000	0.007	0.010	0.012	0.015	0.021	0.009	0.011	0.004
Mg	5.583	5.530	45.152	5.535	5.393	5.347	5.455	5.306	5.275	5.287	5.307	5.273	5.303
Ca	0.000	0.015	0.047	0.007	0.001	0.000	0.002	0.000	0.011	0.002	0.010	0.000	0.000
Cr	0.028	0.000	0.040	0.004	0.004	0.000	0.000	0.006	0.002	0.000	0.001	0.000	0.010
V	0.000	0.008	0.029	0.009	0.000	0.007	0.004	0.002	0.010	0.008	0.000	0.016	0.005

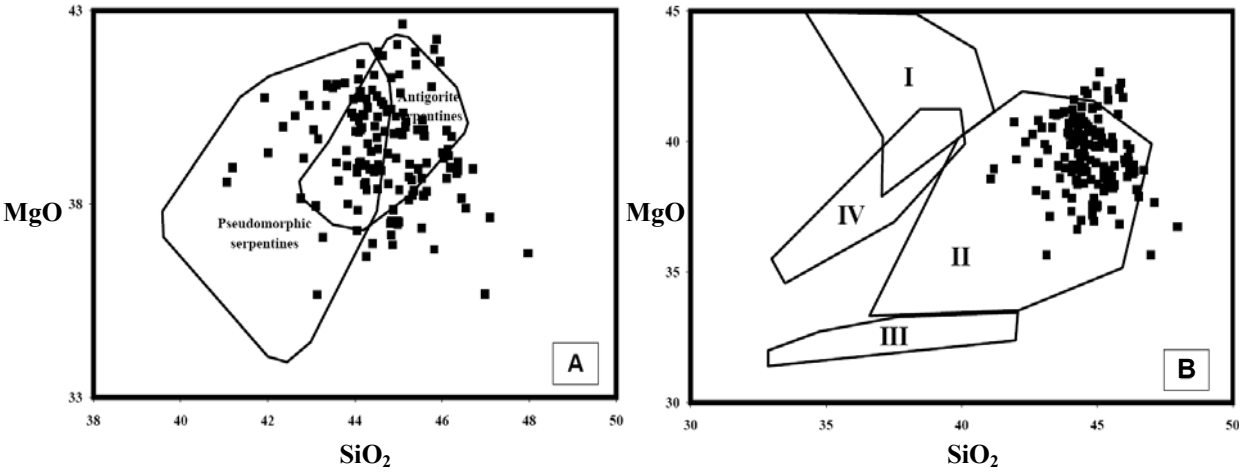

Fig.4: **A)** MgO versus SiO_2 for the analyzed serpentine minerals. Field of Pseudomorphic serpentines and Antigorite serpentinite (after Dungan, 1979)
B) MgO versus SiO_2 for the analyzed serpentine minerals. The fields **I**: Lizardite after magmatic olivine, **II**: Antigorite with interpenetrating texture, **III**: Antigorite with hourglass texture, **IV**: Lizardite after metamorphic olivine (after Wicks and Plant, 1979)

Electron microprobe profile along different serpentine polymorphs shows that there is variation in the concentration of elements (Fe and Mg) in serpentine polymorph along the profile (Fig.6). Antigorite clearly shows higher concentration of FeO and low MgO as compared to lizardite – chrysotile serpentine polymorphs. No distinction between lizardite and chrysotile is plausible. This is because the MgO – SiO_2, FeO – MgO and FeO – SiO_2 contents are approximately the same amount of these oxides, the identification of lizardite from chrysotile is by the Al-content; Chrysotile contains high Al_2O_3 and FeO than lizardite.

BSE analyses show that the intensity of reflected light is directly proportional to the concentration of Fe in the minerals structure (Hamlyan, 1975 and Farahat, 2008). The Fe-rich mineral associates, such as chromian spinel gives light bright color, while Fe-poor olivine and pyroxene give dark gray color in BSE. Antigorite give light gray color (Fig.6A, B and C) due to high Fe content, as compared to other serpentine polymorphs. Chrysotile and antigorite give light gray color; this is because they have low Fe content. Therefore, they are undistinguishable in BSE. In addition, Antigorite is identified from chrysotile by the crystal habits. Whereas, the later is identified by fibrous habits (Fig.7E), while the former is characterized by planet granular habit (Fig.7A, B and C). Lizardite has dark gray color in BSE (Fig.7E) owing to has high Mg and low Fe content. Based on the intensity of reflected light in BSE we can arrange the serpentine minerals in BSE from light gray color to dark gray as follow: antigorite (light gray), chrysotile (intermediate), and lizardite (dark gray).

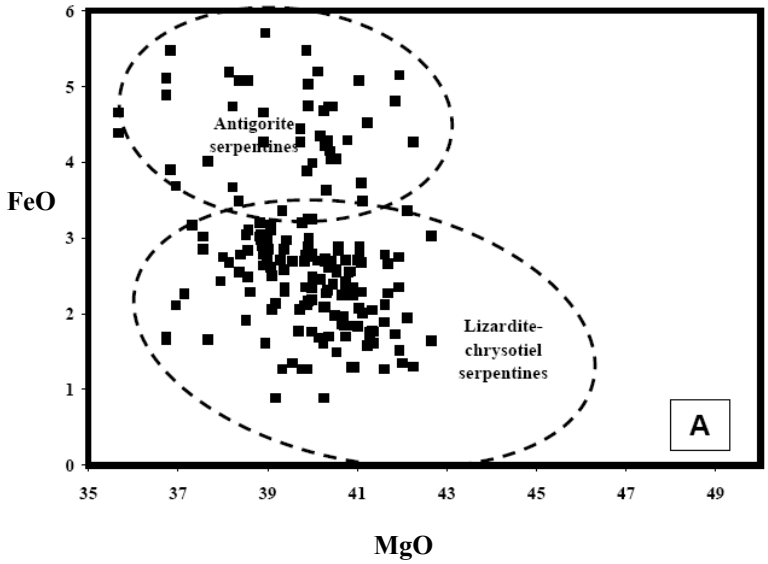

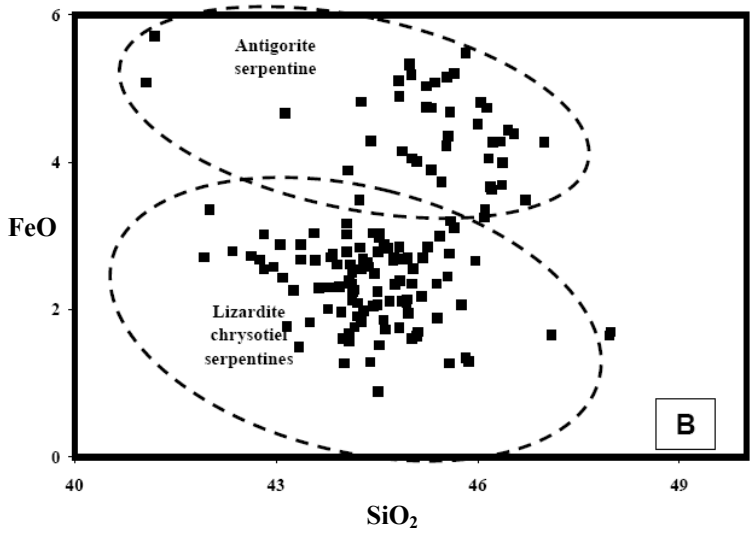

Fig.5: **(A)** FeO versus MgO for the analyzed serpentine minerals.
(B) FeO versus SiO_2 for the analyzed serpentine minerals

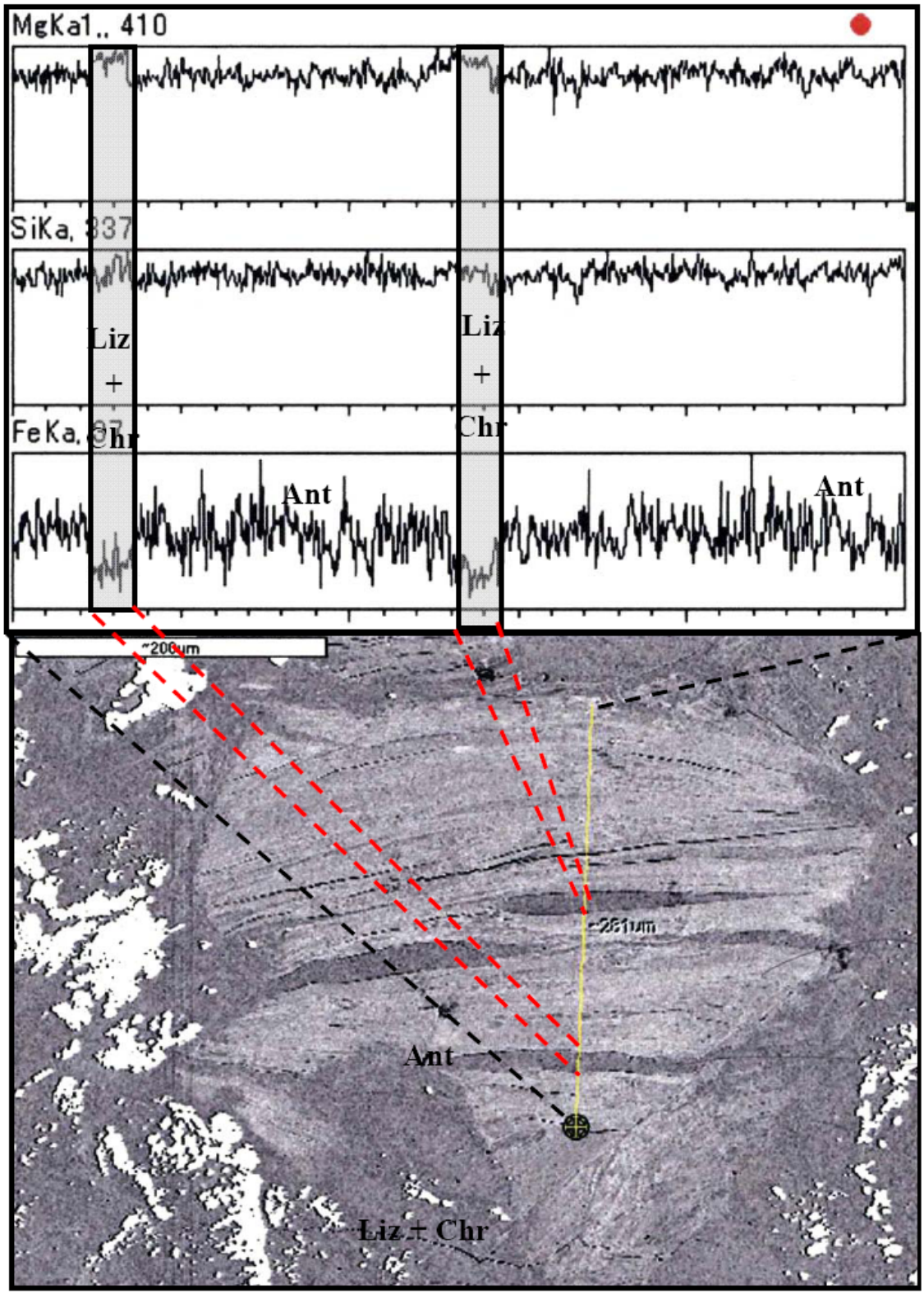

Fig.6: Line scan profile of antigorite in sheared serpentinite showing the enrichments of both Fe and Mg, as compared to lizardite – chrysotile mixture

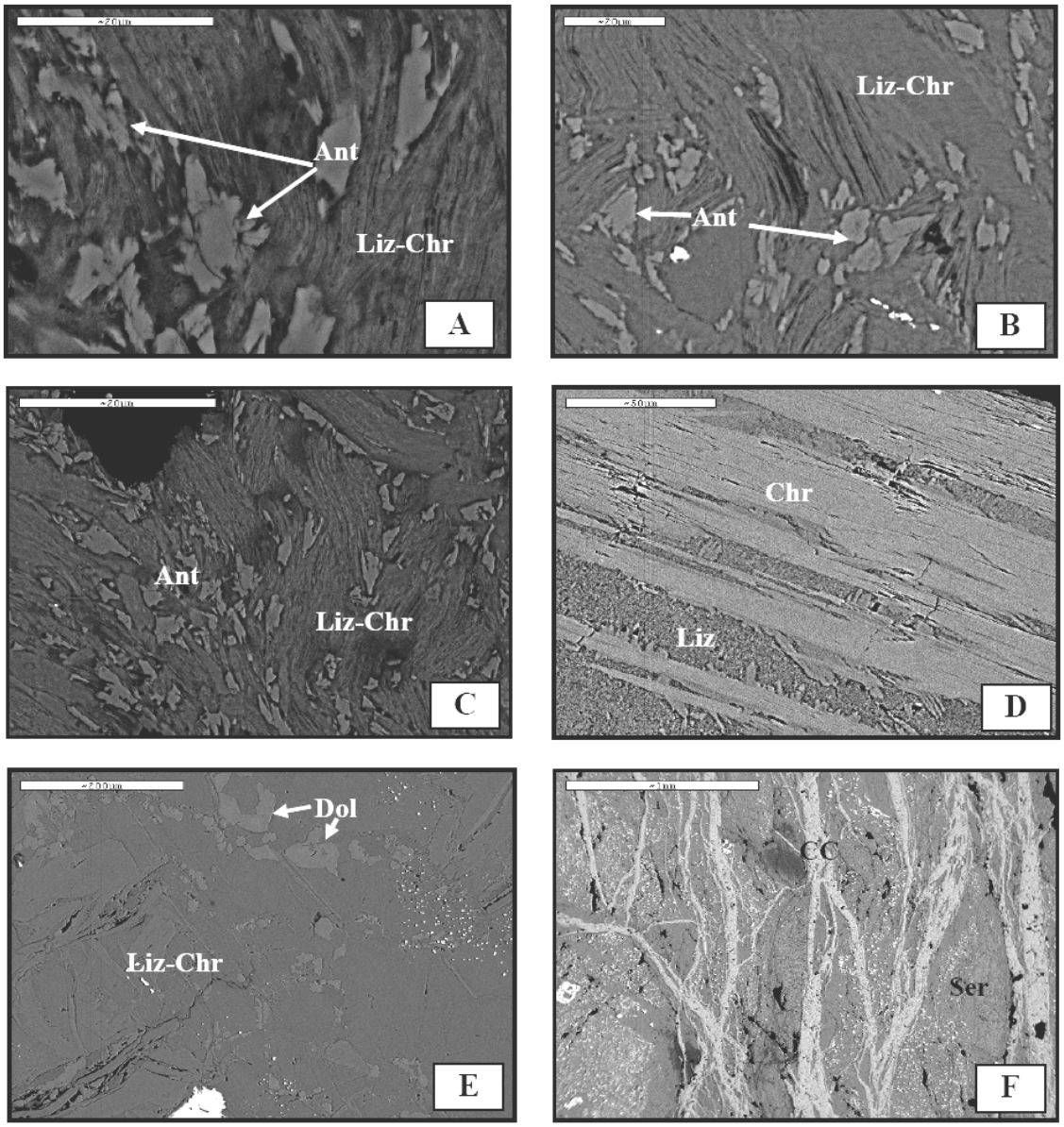

Fig.7: Back-scattered electron images of sheared serpentinite showing different types of serpentine minerals:

A) Light gray planer antigorite with light gray fibrous chrysotile
B) Light gray planer antigorite with light gray fibrous chrysotile and fine dark gray vein of lizardite
C) Schistosity or parallel arrangement in serpentine minerals
D) Fibrous light gray chrysotile with vein of fine grained dark gray lizardite
E) Ductile deformation (bending) in serpentine minerals
F) Tiger skin texture of shear serpentinite with veins of calcite and serpentine

Based on aforementioned evidence and taking into consideration that in MSH (MgO – SiO_2 – H_2O) system, antigorite is stable in higher temperature condition (200 – 600)° C than lizardite and chrysotile serpentine. Lizardite and chrysotile are formed directly from olivine and pyroxene at temperature below 300° C (O'Hanly, 1995). Generally, antigorite forms at the expense of lizardite and/ or chrysotile in the boundary of green schist facies although this transition has an overlapping spectrum depending on composition (Fe content), oxygen fugacity (content of Fe^{2+} and Fe^{3+}) and buffered H_2O (Coleman, 1977). Green schist facies has not been observed in the studied antigorite due to rather low oxygen fugacity. It seems to be that more important is the influence of FeO, because the olivine + talc assemblage has a lower Mg/Fe ratio than coexisting antigorite, the equilibrium temperature of the natural assemblage would have been lower than in the pure MSH system. Page (1967) and Eckstrand (1975) have recognized an increase in the production of magnetite in the advanced stages of serpentinization. In his detailed study of the Burro mountain's peridotite, Page (1967) noted that slightly serpentinized rocks contain high-Fe serpentine with a relatively restricted compositional range. Serpentine in completely hydrated rocks have lower and more variable iron contents. Based on FeO content, *m*-value, oxygen fugacity and water activity, it is found that the studied antigorite is formed at lower metamorphic grade than in the pure MSH system and its formation required shear stress condition. The co-existing of high-Fe antigorite with lizardite – chrysotile assemblages may suggest that the former is stable in slightly higher temperature condition (>300° C) than lizardite and chrysotile serpentine. The absence of dynamo thermal sole in tectonic contact between the sheared serpentinite and the Tertiary molasses (Miocene Merga Red Beds) suggests that metamorphism took place during Miocene post-collision tectonics.

▪ Chromian Spinel

The chemical compositions of spinel are given in Table (2). The composition of chromian spinel display three compositional zonation from core to the rim, as follows: core of the chromian spinel grain, which represents the primary chromian spinel composition with Cr ≠ (Cr/ Cr + Al) 0.6 – 0.7, transitional ferrichromite zone characterized by progressive enrichment in Fe^{2+} and Fe^{3+} and depletion in Mg and Al with Cr ≠ (Cr / Cr + Al) 0.7 – 0.9; and Cr-magnetite rim characterized by extensive enrichment of Fe^{3+}, Fe^{2+} and extensive depletion in Al and Mg. These three stages are represented by primary Cr-spinel, pre-serpentinization spinel and syn-or post-serpentinization spinel, respectively. Based on the chemical characteristic of primary chromian spinel, the tectonic affinity is within for-arc setting of peridotite protoliths (Mohammad, 2008), pre-serpentinization Cr-spinel composition is result of re-equilibration processes down to 500° C that severely affect the Fe – Mg distribution between olivine and primary Cr-spinel. The secondary Cr-spinels point to retrograde metamorphic (i.e. pre and syn-serpentinization) paths resulting from continuous tectonic evolutions during slow uplifting of mantle wedge (Aziz, 2008 and Ahmed *et al.* 2001) concluded that chromian-spinel changes its composition to ferrichromite at higher temperature metamorphism and to Cr-magnetite at low temperature metamorphism.

In BSE of chromian spinel all three zones are recognized, as shown in Fig. (8A and B). The core of chromian spinel is characterized by gray color due to the enrichment in Mg compared to Fe, transitional ferrichromite zone is dark-gray due to the enrichment of Fe^{3+} and Fe^{2+} on the expense of Mg and Cr-magnetite zone is characterized by bright light gray due to extensive enrichment in Fe^{3+}, slight increase in Fe^{2+} and extensive depletion of Al and Mg.

▪ Chlorite

Chlorite (with Cr-magnetite) either encircles the chromian spinel (Fig.8C) or present as inclusions within the ferrichromite forming lamellar texture (Fig.8E). Based on the classification of Hey (1954), all analyzed chlorites are clinochlorite (Fig.9). The latter, to first approximation, has a contact composition $Mg_{9.77}Fe_{0.49}Al_{3.00}Cr_{0.22}Si_{6.4}(OH)_{16}$. Chlorite, which flanks Cr-spinel, however, has high amount of Al_2O_3 and Cr_2O_3. It contains considerable amount of Cr_2O_3 (1.4 – 2.6%) (Table 3) and therefore, it can be referred to as Cr-rich clinochlorite. Cr-spinel is either flanked by or forms with chlorite a polycrystalline aggregate. Therefore, Cr-spinel is the only mineral that could supply Al and Cr in ultramafic system (SiO_2 – CaO – MgO and SiO_2 – MgO – CaO – H_2O system) during serpentinization processes to newly formed chlorite. The trivalent cations (Cr and Al) enrichments in chlorite could be explained according to the following equations:

$AlCrFe^{3+}$ in (Cr-spinel) = Al in (chlorite)-$Fe^{3+}Cr$ in (ferrichromite) …….(1)
$Fe^{3+}Cr$ in (ferrichromite) = Cr in (chlorite)-Fe^{3+} in (magnetite) ……(2)

Investigation of Mellini *et al.* (2005) based on textural evidence, chlorites in serpentinite is a product of Cr-spinel reaction with already formed serpentine supporting this reaction by indicating chlorite aureole separating Cr-spinel from mesh textured serpentines.

MAl_2O_3 (spinel) + 1.5 $M_3SiO_2O_5$ $(OH)_4$ (serpentinite) + H_2O + $0.083O_2$ =
M_5AlAl Si_3O_{20} $(OH)_8$ (chlorite) + M_3O_4 (magnetite)……(3)
M= Mg, Fe^{2+}, Fe^{3+}

As the aluminum of clinochlore is sensitive to temperature (and independent of pressure), remaining essentially constant (2 Al atoms/formula unit) below at 700° C, and increasing to (2 – 4) 2 Al atoms/formula unit by its breakdown temperature (Jenkins and Chernosky, 1986). The clinochlore in the studied serpentinite is approximately equal to 3 Al atoms/formula units. This may suggest that the ferichromite – clinochlore assemblages are related to pre-serpentinization re-equilibration.

$2MgAl_2O_4$ (spinel) + $2Mg_2SiO_4$ (olivine) + $2Mg_2Si_2O_6$ (enstatite) + $8H_2O$ =
$Mg_{10}Al_2Al_2Si_6O_{20}$ $(OH)_{16}$ (chlorite)……..…(4)

The aforementioned equation stated above elucidates that the Cr-spinels zonation (i.e. chromian core and ferichromite rim) point to pre-serpentinization metamorphic path resulting from continuous evolutions during the slow uplifting of mantle-wedge.

▪ Carbonate Minerals

The representative chemical compositions of carbonate are given in Table (4). The chemical composition indicates that they consist of both dolomite and aragonite. Dolomite is characterized by high MgO content, about 20 wt.% and FeO does not exceed 1.3%, whereas in aragonite the amount of MgO does not exceed 1.5 wt.% and FeO is less than 0.1 wt.%. In BSE, dolomite occurs as granular grain within serpentine minerals (Fig.7F) and characterized by light gray color, while aragonite occurs as band or vein filling (Fig.7G) between serpentine minerals and gives light color in BSE. The magnesium content of calcite coexisting with dolomite forms the basis of geo-thermometer, which as Goldsmith and Newton (1969) have shown, is relatively independent of pressure. Equilibrium temperature is estimated from compositions of coexisting calcite + dolomite by determining the $MgCO_3$ ($XMgCO_3$ 2.7 – 3.2%) content in calcite is below 500° C.

Table 2: Representative micro analyses of chromian spinel from sheared serpentinite

	Rim			Core						Transitional zone		
Oxides (wt.%)												
SiO_2	0.07	0.21	0.08	0.12	0.11	0.24	0.09	0.05	0.05	0.11	0.00	0.06
TiO_2	0.22	0.21	0.18	0.28	0.41	0.29	0.33	0.42	0.31	0.55	0.14	0.18
Al_2O_3	0.14	0.10	0.09	19.24	18.76	18.45	20.27	18.34	15.68	15.87	12.79	13.35
Fe_2O_3	60.33	61.55	58.86	8.20	8.41	6.58	7.42	6.06	8.85	8.89	2.62	3.00
FeO	28.16	28.87	27.25	19.47	19.78	19.70	18.81	20.27	20.60	20.47	22.09	22.56
MnO	0.12	0.42	0.49	0.98	0.83	1.03	0.86	1.01	0.89	1.01	0.48	0.72
MgO	0.64	0.43	0.69	7.54	7.08	7.79	8.28	7.59	6.33	6.39	6.82	6.87
Cr_2O_3	3.82	2.10	7.11	42.38	41.46	43.82	42.29	43.88	42.41	42.78	52.80	52.40
V_2O_5	0.12	0.29	0.18	0.20	0.31	0.52	0.28	0.29	0.39	0.29	0.35	0.52
NiO	0.50	0.29	0.50	0.00	0.00	0.31	0.07	0.00	0.18	0.36	0.00	0.00
Total	94.15	94.51	95.76	99.28	98.12	99.50	99.61	98.48	96.36	97.45	98.41	100.05
Cation proportions per 4 oxygen atoms												
Si	0.003	0.009	0.003	0.004	0.004	0.008	0.003	0.002	0.002	0.004	0.000	0.002
Ti	0.007	0.006	0.005	0.007	0.010	0.007	0.008	0.010	0.008	0.014	0.004	0.005
Al	0.007	0.005	0.004	0.733	0.725	0.703	0.763	0.708	0.630	0.630	0.510	0.522
Fe^{3+}	1.842	1.876	1.759	0.200	0.208	0.160	0.178	0.149	0.227	0.225	0.067	0.075
Fe^{2+}	0.956	0.978	0.905	0.526	0.543	0.533	0.502	0.555	0.587	0.576	0.625	0.626
Mn	0.004	0.014	0.016	0.027	0.023	0.028	0.023	0.028	0.026	0.029	0.014	0.020
Mg	0.039	0.026	0.041	0.363	0.346	0.375	0.394	0.370	0.321	0.321	0.344	0.340
Cr	0.123	0.067	0.223	1.083	1.075	1.120	1.068	1.136	1.142	1.138	1.411	1.375
V	0.003	0.008	0.005	0.004	0.007	0.011	0.006	0.006	0.009	0.006	0.008	0.011
Ni	0.016	0.009	0.016	0.000	0.000	0.008	0.002	0.000	0.005	0.010	0.000	0.000
Cr ≠	0.95	0.93	0.98	0.60	0.60	0.61	0.58	0.62	0.64	0.64	0.73	0.72

Table 3: Representative micro analyses of chlorite from sheared serpentinite

	Chlorite											
Oxides (wt.%)												
SiO_2	33.42	33.55	33.57	33.30	33.34	33.44	34.21	35.27	35.37	34.37	35.35	35.45
TiO_2	0.00	0.00	0.00	0.00	0.04	0.10	0.00	0.03	0.00	1.55	0.20	0.06
Al_2O_3	13.27	13.27	13.22	13.26	13.34	13.37	17.55	15.15	14.91	13.52	14.05	13.68
Fe_2O_3	0.00	0.00	0.00	0.00	0.00	0.00	0.00	0.00	0.00	0.00	0.00	0.00
FeO	3.07	2.99	2.73	2.73	2.66	2.62	2.36	1.85	2.43	1.70	2.11	2.27
MnO	0.19	0.19	0.22	0.22	0.20	0.19	0.00	0.00	0.00	0.86	0.00	0.00
MgO	34.22	34.64	34.48	34.70	35.01	34.92	36.14	36.37	36.84	35.01	35.42	35.57
Cr_2O_3	1.42	1.43	1.43	1.43	1.58	1.51	1.45	1.38	1.25	2.44	1.41	1.32
V_2O_5	0.14	0.08	0.05	0.11	0.04	0.05	1.73	0.37	0.13	0.00	0.00	0.00
Total	85.77	86.26	85.82	85.77	86.27	86.27	91.71	90.25	90.97	89.45	88.65	88.49
Cation proportions per 28 oxygen atoms												
Si	6.40	6.40	6.42	6.38	6.35	6.37	5.99	6.35	6.35	6.32	6.50	6.54
Ti	0.00	0.00	0.00	0.00	0.01	0.01	0.00	0.00	0.00	0.21	0.03	0.01
Al	3.00	2.98	2.98	2.99	3.00	3.00	3.62	3.21	3.16	2.93	3.05	2.97
Fe^{3+}	0.00	0.00	0.00	0.00	0.00	0.00	0.00	0.00	0.00	0.00	0.00	0.00
Fe^{2+}	0.49	0.48	0.44	0.44	0.42	0.42	0.35	0.28	0.36	0.26	0.32	0.35
Mn	0.03	0.03	0.04	0.04	0.03	0.03	0.00	0.00	0.00	0.13	0.00	0.00
Mg	9.77	9.84	9.83	9.90	9.94	9.91	9.43	9.76	9.86	9.60	9.71	9.78
Cr	0.22	0.22	0.22	0.22	0.24	0.23	0.20	0.20	0.18	0.35	0.21	0.19
V	0.02	0.01	0.01	0.01	0.01	0.01	0.20	0.04	0.02	0.00	0.00	0.00

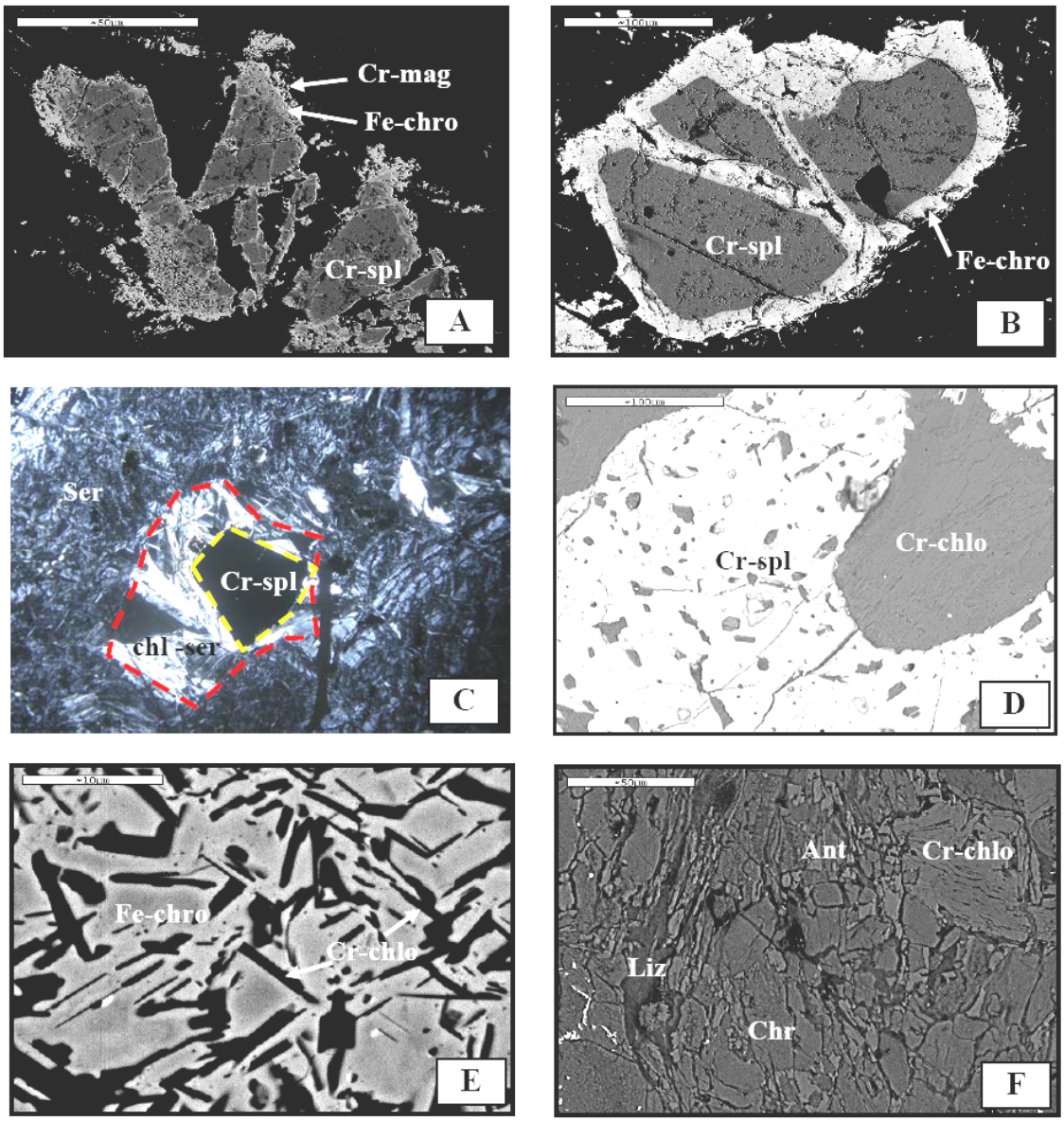

Fig.8: Back-scattered electron images of sheared serpentinite showing replacement of chromian spinel by ferichromite, Cr-magnetite and chromium chlorite:

A) Alteration along fracture in chromian spinel
B) Advanced alteration with sharp, lobate boundaries between dark gray core and light gray ferrichromite with thin rim of Cr-magnetite
C) Concentric alteration in chromian spinel with unaltered dark gray core through transitional light gray ferrichromite to thin rim of light Cr-magnetite
D) Core of chromian spinel grain replaced by chromian chlorite during amphibolite facies
E) Acicular dark clinochlorite occupied the entire area of chromian spinel
F) Fibrous chromian clinochlorite with serpentine minerals

Table 4: Representative micro analyses of carbonate minerals from sheared serpentinite

	Dolomite						Calcite					
Oxides (wt.%)												
SiO_2	0.13	0.09	0.08	0.19	0.14	0.00	0.00	0.11	0.14	0.12	0.12	0.07
Fe_2O_3	0.00	0.00	0.00	0.00	0.00	0.00	0.00	0.00	0.00	0.00	0.00	0.00
FeO	1.28	1.24	1.25	0.49	0.97	0.83	0.00	0.11	0.15	0.03	0.00	0.00
MnO	0.16	0.20	0.23	0.00	0.00	0.04	0.34	0.05	0.00	0.00	0.06	0.06
MgO	20.16	19.99	19.94	21.02	20.00	19.38	1.06	1.27	1.21	1.23	1.22	1.21
CaO	29.26	29.35	29.38	30.49	29.23	29.26	52.43	52.12	51.76	52.13	52.35	52.34
Total	51.17	51.1	51.1	52.97	50.52	49.54	54.36	54.06	53.54	53.78	53.95	53.89
Cation proportions per 6 oxygen atoms												
Si	0.012	0.009	0.008	0.017	0.013	0.000	0.000	0.011	0.014	0.012	0.012	0.007
Fe^{3+}	0.000	0.000	0.000	0.000	0.000	0.000	0.000	0.000	0.000	0.000	0.000	0.000
Fe^{2+}	0.102	0.098	0.099	0.037	0.078	0.068	0.000	0.009	0.013	0.003	0.000	0.000
Mn	0.013	0.016	0.019	0.000	0.000	0.003	0.029	0.004	0.000	0.000	0.005	0.005
Mg	2.853	2.830	2.826	2.852	2.852	2.841	0.159	0.193	0.186	0.189	0.187	0.186
Ca	2.976	2.987	2.993	2.974	2.996	3.083	5.665	5.691	5.716	5.744	5.760	5.771

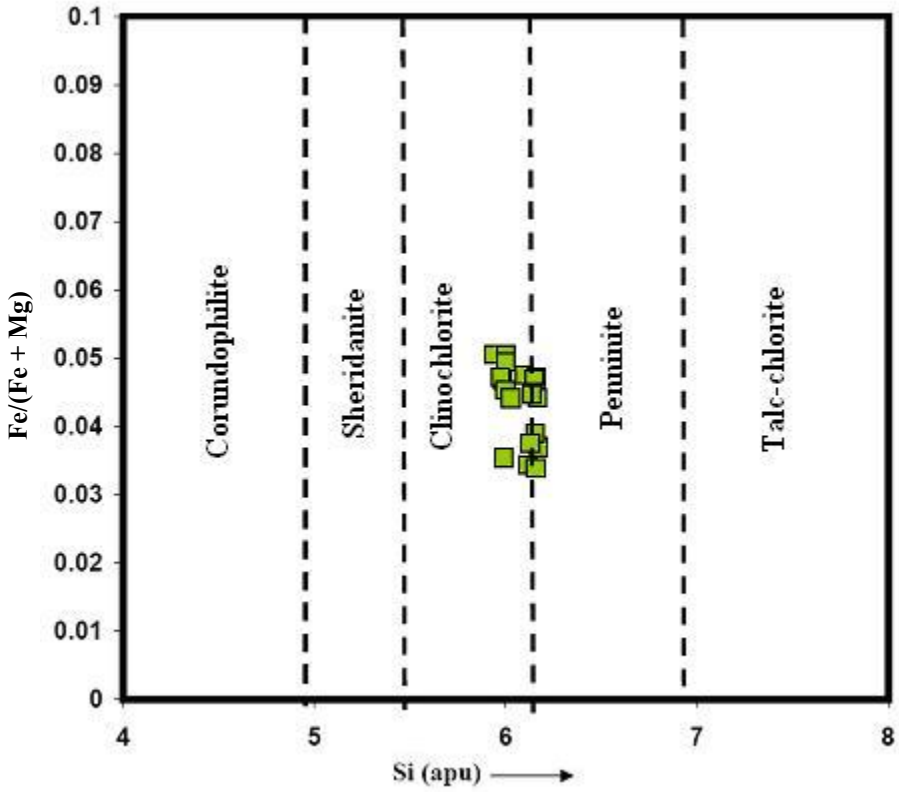

Fig.9: Composition of chlorite in sheared serpentinite plotted on chlorite classification diagram (after Hey, 1954)

CONCLUSIONS

- The investigated 2 meter thick serpentinite occur as peripheral serpentinite rocks along main thrust fault between Penjween igneous body and Merga Red Bed Series, it is a part of main massive serpentinite body.
- Massive serpentinite is transformed to sheared serpentinite due to local rising of pressure along the main thrust fault.
- Based on microscopic observation, microprobe analyses and BSE analyses, sheared serpentinite consists of serpentine polymorph (mainly antigorite, lizardite chrysotile) +

chromian spinel + chromian chlorite + carbonate minerals. Massive serpentinite is transformed to antigorite schist, which represents ductile – brittle deformation under high pressure – temperature condition.

- The best way for identification of serpentine polymorph is using BSE analyses of serpentine polymorphs.
- Chrysotile exhibited as fibrous serpentine polymorph with light gray color, lizardite exhibited as fine grain serpentine polymorph with dark-gray color and antigorite exhibited planer granular light-gray color serpentine polymorphs.
- The chemical analysis of serpentine polymorph shows that the antigorite is richer in FeO and poorer in MgO and SiO_2 than in lizardite – chrysotile serpentines. In addition chrysotile contain about (2 – 3) % of Al_2O_3, which possibly indicates that it is formed after pyroxene.
- The occurrence of carbonate minerals are related to late carbonization of serpentinite due to influx of fluid containing more than 5% of CO_2.
- The formation of chromian clinochlorite is represented by two stages, first generation chlorite as inclusions in chromian spinel are of upper mantel origin, which is formed during interaction chromian spinel with silicate phase in hydrous condition. Second stage chlorite as auroule around chromian spinel or ferichromite represent low temperature hydrothermal reaction between chromian spinel and already formed serpentine minerals.

ACKNOWLEDGMENTS

The authors thank Prof. K.J. Aswad and Dr. M.M. Al-Quaze for their constructive reviews and comments. Dr. K.H. Karim is highly appreciated for his valuable comments on the early version of the manuscript.

REFERENCES

Al-Hassan, M.I., 1975. Comparative petrologic study between Mawat and Penjween igneous complexes, Northeastren Iraq. Unpub. M.Sc. Thesis, University of Baghdad, 114pp.

Al-Hassan, M.I., 1982. Petrology, mineralogy and geochemistry of the Penjween igneous complexes, Northeastern Iraq. Unpub. Ph.D. Thesis, University of Dunde.

Auzende, A.L., Guillot, S., Devouard, B., Barnnet, A. and Daniel, I., 2003. Antigorite microstructure in alpine serpentinite: A record of metamorphic conditions?. Geophysical Research Abstracts, Vol.5, 10566.

Ahmed, H.A., Arai S. and Attia, A.l.K., 2001. Petrological characteristics of podiform chromitites and associated peridotites of the Pan African Proterozoic Ophiolite complexes of Egypt. Mineralum Deposita, Vol.36, p. 72 – 84.

Aqrawi, A.M., Elias, M.E. and Mohammad, Y.O., 2007. Oxygen and hydrogen isotope study of serpentinized peridotite rocks, Thrust Zone, North Eastern Iraq. Iraqi Jour. Earth Sci., Vol.1, p. 13 – 20.

Aswad, K.J. and Elias, E.M., 1988. Petrogenesis, geochemistry and metamorphism of spilitized subvolcanic rocks of the Mawat Ophiolite complex, NE Iraq. Ofiolitti, Vol.13, No.2/3, p. 95 – 109.

Aswad, K.J., 1999. Arc-continent collision in Northeastren Iraq as evidenced by Mawat and Penjween Ophiolite complex. Raf. Jour. Sci., Vol.10, No.1, p. 51 – 61.

Aziz, N.R., 2008. Petrogenesis, Evolution and Tectonics of the Serpentinites of the Zagros Suture Zone, Kurdistan Region, NE Iraq. Unpub. Ph.D. Thesis, University of Sulaimaniyah, Iraq. 210pp.

Chapman, J.A. and Zussman, J., 1959. Further electron optical observations on crystals of antigorite. Acta Crystallographic, Vol.12, p. 550 – 552.

Coleman, R.G., 1977. Ophiolites: Ancient Oceanic Lithosphere?. Springer Verlag, 229pp.

Droop, G.T.R., 1987. A general equation for estimating Fe^{+3} concentrations in ferromagnesian silicates and oxides from microprobe analyses, using stoichiometric criteria. Mineralogical Magazine, Vol.51, p. 431 – 435.

Dungan, M.A., 1979. A microprobe study of antigorite and some serpentine pseudomorphs. Canadian Mineralogist, Vol.17, p. 711–784.

Eckstrand, O.R., 1975. The Dumont serpentinite: A model for control of nickeliferous opaque mineral assemblages by alteration reactions in ultramafic rocks. Economic Geology, Vol.70, p. 183 – 201.

Farahat, E.S., 2008. Chrome-spinels in serpentinites and talc carbonates of the El Ideid-El Sodmein District, Central Eastern Desert, Egypt: Their metamorphism and petrogenetic implications. Chemie der Erde-Geochemistry, Vol.68, p. 193 – 205.

Goldsmith, J.R. and Newton, R.C., 1969. P – T – X relations in the system $CaCO_3$ – $MgCO_3$, at high temperatures and pressures. American Jour. Sci., Vol.67A, p. 160 – 190.

Hamlayn, P.R., 1975. Chromite alteration in the Panton Sill, East Kimberley Region, Western Australia. Mineralogical Magazine, Vol.40, p. 181 – 192.

Hey, M.H., 1954. A further note on the presentation of chemical analyses of minerals. Mineralogical Magazine, Vol.30, p. 481 – 497

Kunze, G., 1956. Die gewellte Struktur des Antigorits. I.Z. Kristallogr, Vol.10, p. 82 – 107.

Kunze, G., 1958. Die gewellte Struktur des Antigoritaes. II.Z. Kristallogr, Vol.110, p. 282 – 320.

Koyi, A.M., 2006. Petrochemistry, petrogenesis and isotope dating of Walash volcanic rocks at Mawat – Chowarta area, NE Iraq. Unpub. M.Sc. Thesis, Mosul University, Iraq, 226pp.

McCarthy, M.J., 1965. Geology of Penjwin area. GEOSURV, manuscript report.

Mahmmod, L.A., 1978. Petrology and geochemistry of ultramafics around Penjween, Northeast Iraq with special reference to the genesis of the chromites associated with them. Unpub. M.Sc. Thesis, Mosul University, 210pp.

Mohammad, Y.O., 2004. Petrology and geochemistry of serpentine and associated rocks in Mawat and Penjween areas, Kurdistan Region, Northeastern Iraq. Unpub. M.Sc. Thesis, University of Sulaimaniyah, 189pp.

Mohammad Y.O., Maekawa, H., 2007. Serpentinite and serpentinization events along the Iraqi Zagros Thrust Zone (IZTZ). Proceedings of Second International Conference on the Geology of the Tethys, University of Cairo, p. 85 – 100.

Mohammad, Y.O., 2008. Petrology of ultramafic and related rocks along Iraqi Zagros Thrust Zone. Unpubl. D.Sc. Thesis, Osaka Prefecture University, Japan, 154pp.

Mellini, M. and Zussman, J., 1986. Carlosturanite (not picrolite) from Taberg, Sweden. Mineralogical Magazine, Vol.50, p. 675 – 679.

Mellini, M., Trommsdorff, V. and Compagnoni, R., 1987. Antigorite polysomatism: Behaviour during progressive metamorphism. Contributions to Mineralogy and Petrology, Vol.97, p. 147 – 155.

Mellini, M., Rumori, C. and Viti, C., 2005. Hydrothermally reset magmatic spinels in retrograde serpentinites: Formation of ''ferichromite'' rims and chlorite aureoles. Contributions to Mineralogy and Petrology, Vol.149, p. 266 – 275.

Nicolas, A., Giradrdeau, J., Marcoux, J., Dupre, B., Xiban, W., Yougong, C., Hiaxing, Z. and Xuchang, X., 1981. The Xigaze Ophiolite (Tibet): A peculiar oceanic lithosphere. Nature, Vol.294, p. 414 – 417.

O'Hanley, D.S., 1992. Serpentinites: Records of Tectonics and Petrological History. Oxford University Press, 269pp.

Page, N.J., 1967. Serpentinization at Burro Mountain, California. Contributions to Mineralogy and Petrology, Vol.14, Issue 4, p. 321 – 342

Piniazkiewicz, J., McCarthy, E.F. and Genco, N.A., 1994. Talc, In: Industrial Minerals and Rocks, 6th Edit., Carr, D.D., (Ed.). Society for Mining, Metallurgy and Exploration, Inc., Littleton, Colorado, p. 1049 – 1069.

Smirnov, V.A., and Nelidove, 1962. Report on 1: 200 000 prospecting correlation of the Sulaimaniyah – Choarta and Penjween area carried out in 1961. GEOSURV, int. rep no. 290.

Spear, F.S., 1994. Metamorphic Phase Equilibrium and Pressure-Temperature-Time Paths. Mineralogical Society of America, Washington, D.C., 799pp.

Uehara, S., 1998. TEM and XRD study of antigorite superstructures. Canadian Mineralogist, Vol.36, p. 1595 – 1605.

Wicks, F.J. and Plant, A.G., 1979. Electron microprobe and X-ray microbeam studies of serpentine textures. Canadian Mineralogist, Vol.17, p. 785 – 830.

Worden, R.H. and Droop, G.T.R., and Champness, P.E., 1991. The reaction antigorite + olivine + talc + H_2O in the Bergell aureole, N Italy. Mineralogical Magazine, Vol.55, p. 367 – 377.

Wunder, B., Wirth, R. and Gottschalk, M., 2001. Antigorite: Pressure and temperature dependence of polysomatism and water content. European Jour. of Mineralogy, Vol.13, p. 485 – 495.